Inversion of Time-Lapse Electrical Resistivity Imaging Data for Monitoring Infiltration

Vanessa Mitchell, Geophysics Department, Stanford University, Adam Pidlisecky, Geosciences Department, University of Calgary, and Rosemary Knight, Geophysics Department, Stanford University*

Summary

We consider two methods for inversion of time-lapse electrical resistivity imaging (ERI) data based on the concept of informed imaging, defined as the incorporation of all prior knowledge about a site into the acquisition, inversion, and interpretation of data. The first method uses a preconditioned conjugate gradient algorithm with a regularization term that incorporates information about the conductivity structure from the preceding time step. The second method uses the extended Kalman Filter (EKF) to invert each imaging experiment given knowledge about model structure and the error structure from all previous imaging experiments. We demonstrate the use of these inversion algorithms on real and synthetic time-lapse data acquired while monitoring infiltration processes in the near surface.

Introduction

Monitoring hydrologic processes in the vadose zone is of great importance in developing management strategies for groundwater resources. Flow and transport behavior in variably saturated media control the rate at which, and path along which, fluids or contaminants reach groundwater aquifers. Electrical resistivity imaging (ERI) is sensitive to changes in the subsurface conductivity structure, which is highly dependent on the water saturation distribution in the vadose zone. Time-lapse ERI, therefore, has been widely used for environmental and hydrologic monitoring experiments.

ERI monitoring of near-surface processes has included tracking infiltration (Daily et al., 1992), estimating transport properties (Binley et al., 2002), and quantifying plume evolution in saturated media (Singha and Gorelick, 2005). In most applications of ERI to environmental monitoring, inversion of time-lapse data has relied on either differential or absolute imaging methods. In differential imaging, data are transformed before inversion by taking the difference or ratio of data collected at later time steps relative to data collected during the initial imaging experiment. The differenced data are then inverted to recover relative log-conductivity values (see e.g. Park, 1998; or Chambers et al., 2004). In absolute imaging each imaging experiment is inverted independently of other data and absolute estimates of the conductivity values are recovered (Zhou et al., 2001). The reference model for starting the inversion in absolute imaging is often the same for each time-step, though the conductivity model from the previous time step has also been used, as in Oldenborger et al. (2007), in which the authors compare absolute and differenced imaging approaches using 3D time-series data for an injection withdrawal experiment in a shallow aquifer.

In this study we use ERI to monitor infiltration beneath the Harkins Slough Recharge Pond (HSRP), part of a coastal aquifer management project in an agricultural region of Northern California. Water diverted to the HSRP is used to recharge the aquifer beneath the pond, slowing saltwater intrusion and supplementing water resources to meet demand during the irrigation season. We consider two methods for inverting the data collected from the study within an informed imaging framework, meaning all existing information about a site and experiment is incorporated into the acquisition, processing and interpretation of ERI data. Both of the approaches applied in this study incorporate information gained from the inversion of data acquired from imaging experiments at earlier time steps into the inversion of data at the current time-step. In the first approach, we use the inverted conductivity model from the previous time step as a reference model for the inversion at the current time-step, incorporated as a regularization term within a Gauss-Newton (GN) inversion algorithm (Pidlisecky et al., 2007). We also propose a stochastic inversion method using the extended Kalman Filter (EKF), which incorporates information about both the evolution of the physical system being monitored and the structure of the model error covariance to update estimates of model parameters. The EKF model updates are recursive; hence, information from all previous time-steps is included in the current update.

Field Experiment

Our primary interest at the HSRP is to image infiltration in the top few meters of the near surface. Prior investigations using 1D electrical resistivity probes recording to a depth of 2 m and grain-size analysis of 5-m cores suggest a 0.5-m thick layer of fines-rich sediment at the surface, with medium to coarse-grained sand below this layer. It is hypothesized that clogging from very-fine particulates in the water column or bioactivity in the fines-rich layer causes an observed decrease in infiltration rate with time, limiting the effectiveness of the pond. However, it may be that infiltration rates are simply limited by the permeability within the top layer, and initial rates are artificially high from tilling of the pond base prior to infiltration. Operators

require a better understanding of flow behavior below the pond to understand the parameters controlling fluid flow in the near surface.

Prior to the diversion period in 2008-2009, electrodes were implanted along a 20-m line at a depth 0.25 m below the base of the pond. Forty electrodes were used with a regular separation of 0.5 m. Using an imaging experiment of 154 Wenner arrays with source-receiver offsets ranging from 0.5 m to 2.5 m, measurements were collected across the length of the line. Imaging experiments were repeated at approximately 1.5-hour intervals for 3 months during the diversion period. Water diversion began approximately 7 weeks (1158 hours) after the start of the monitoring experiment. A number of power surges resulted in incomplete or lost data, resulting in a total of 1936 complete data sets over approximately 19 weeks (3080 hours).

Inversion Methods

For the first inversion approach, we use a 2D version of the GN algorithm presented by Pidlisecky et al. (2007). This application uses two-grids in the model update. At each iteration, a 'fine' grid of 318 by 124 cells is used to calculate the Jacobian, the sensitivity of measurements to changes in model parameters, and predicted data, and a 'coarse' grid of 147 by 51 cells is used to estimate model parameters. Multiple grids are used to improve estimates of the Jacobian, especially near source locations, while limiting the number of model parameters; this combination increases the stability of the inversion process. The model update at each iteration is estimated using a precondition conjugate gradient (PCG) algorithm.

We incorporate information derived from the inversion of data from previous imaging experiments through a regularization term. Within the objective function of the inversion, the regularization term penalizes large differences between the current estimated model and a reference model, taken here to be the inverted conductivity structure from the previous time step. Inclusion of the regularization term incorporates our knowledge that the short sampling interval, relative to the time-scale at which the water moves through the subsurface, means there are only small variations between adjacent imaging experiments; i.e. the conductivity structure at the current time-step should be very close to the conductivity structure at the preceding time-step. In addition to this explicit regularization, the PCG algorthim is solved to a low tolerance, which results in further model regularization.

The second approach uses a stochastic framework to incorporate previous knowledge through the use of the extended Kalman Filter (EKF). Kalman (1960) first proposed a prediction-filter method for evaluating time-series stochastic data that incorporates knowledge acquired from all previous time-steps to estimate parameters at the current time-step. This method is based on iterative updates to the expression describing the evolution of the measured physical system and the measurement process. The EKF is a modified version of the original Kalman Filter that is adapted to predict and filter nonlinear processes. We follow here the derivation of the EKF presented by Leikhoinen et al. (2009), who were the first to apply the EKF to electrical resistivity monitoring data. In their study they consider a cross-borehole configuration for imaging infiltration with a 24-hour sampling interval. We adapt the method for our application of dense temporal sampling of an infiltration experiment using surface-based ERI. For our experiment we alter the update of the physical state being monitored at each time-step. Furthermore, we must consider that our data resolution will be decreased as a result of the acquisition geometry.

We consider a system of two stochastic processes describing the evolution of the physical system (the state equation) and the measurement process (the observation equation). These are represented by (1) and (2), respectively.

$$\sigma_{k+1} = \mathbf{F}_k \sigma_k + \omega_k \quad (1)$$

$$U_k = \mathbf{V}_k(\sigma_k) + \upsilon_k \quad (2)$$

In this representation, σ is an m-dimensional vector of model parameters (the conductivity values); **F** is the state update matrix; U is the n-dimensional vector of measurements (potential differences); **V** is the operator describing the measurement process; and k is the time index. The vectors ω and υ are stochastic noise components with 0-mean and variances s_ω^2 and s_υ^2, respectively. Linearization of the expression for the measurement process about the current time-step has the form $Uk \sim \mathbf{V}_k(\sigma_{k-1})+J_k(\sigma_k- \sigma_{k-1})+\varepsilon_k$. The prediction-update iterations for each new measurement then have the form:

$$\sigma_{k|k-1} = \mathbf{F}_{k-1}\sigma_{k-1} \quad (3)$$

$$\Gamma_{k|k-1} = \mathbf{F}_k \Gamma_{k-1} \mathbf{F}_k^T + \Gamma^{\omega}_{k-1} \quad (4)$$

$$G_k = \Gamma_{k|k-1} H_k^T \left(H_k \Gamma_{k|k-1} H_k^T + \Gamma_k^{\varepsilon} \right) \quad (5)$$

$$\Gamma_{k|k} = \left(I - G_k H_k \right) \Gamma_{k|k-1} \quad (6)$$

$$\sigma_{k|k} = \sigma_{k|k-1} + G_k \left(y_k - H_k \sigma_{k|k-1} \right) \quad (7)$$

where

$$\Gamma_k^i = s_i^2 \mathbf{I}\,, \quad (8)$$

$$y_k = \begin{pmatrix} U_k - V_k(\sigma_{k|k-1}) + J_k \sigma_{k-1} \\ \alpha R \sigma_* \end{pmatrix}, \quad (9)$$

and

$$H_k = \begin{pmatrix} J_k \\ \alpha R \end{pmatrix}. \qquad (10)$$

Equation (8) is the error covariance matrix, where *i* can be ε, or ω. The first terms in equations (9) and (10) describe the data misfit between the predicted and observed data based on the linearized expression of the measurement process. The second terms represent regularization of the model solution, where α is a weighting parameter, *R* is a smoothing operator and σ_* is a reference conductivity model.

Equations (3) and (4) are predictions of the conductivity model and the model error covariance based on data acquired up to the k-1 time-step. Equations (5)-(7) filter the predictions based on the most recent observed data. In this application, where we assume very dense temporal sampling, we can approximate the state evolution as a simple linear process, rather than a nonlinear process as assumed in the original derivation. Our linear assumption is consistent with similar applications of electrical impedance tomography used in medical imaging (Vaukhonen et al., 1998; and Kim et al., 2002). Another important difference in our application is that we are working with surface ERI data, not cross-borehole data. Although the acquisition geometry does not change the form of the prediction-filter equations above, it has important implications for measurement resolution of our data.

Inversion Results using the GN-Algorithm

Using the GN algorithm described above, we invert the time-series data acquired at the pond. The time-lapse imaging data from each time-step are inverted to a tolerance of 4.5% with a maximum of 10 iterations and a reference model, after the initial time step, equal to the solution at the previous time step. The reference model for the initial time-step is a simple, layered conductivity model. If the misfit between the predicted data and observed data is less than the tolerance at the initial iteration for an imaging experiment, the inversion process is skipped and the model remains unchanged. A number of inverted models from different time-steps are included as Figure 1. The results are presented as relative differences with respect to the initial imaging experiment to better show changes in the estimated structure. The inverted conductivity models clearly show wetting from a rain event at ~300 hours, followed by drying back to initial subsurface conditions prior to the diversion of water to the pond. After diversion begins at 1160 hours, however, the models again show alternating periods of wetting and drying in the deeper sediments, but the hydraulic head in the pond remains relatively constant until monitoring ends. The inverted conductivity models indicate a complex infiltration process that cannot be explained by a simple model of clogging in the fines-rich layer as initially predicted.

Although the amount of spurious noise and structure introduced into the model is limited by only processing data with variation above the misfit tolerance, the inversion results still become noisy after a large number of time-steps using this method. Resetting the reference model to the initial reference model after ~200 inversions and proceeding with the method as described above does help to limit this effect. However, this behavior highlights some of the challenges of using this method: 1) weighting the reference model relative to the data misfit to find the appropriate balance of informing the inversion through previous information and allowing variations in data to drive the inversion process, and 2) limiting the introduction of artifacts into the model estimates from the inversion process.

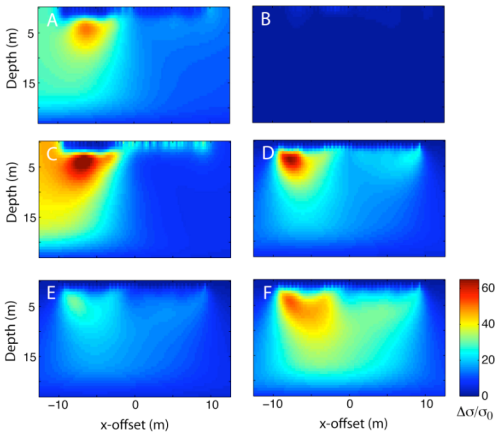

Figure 1: Six time-lapse relative difference conductivity structures with respect to the initial conductivity model inverted using GN-algorithm. A: 325.5 hours (rain event); B: 627 hours; C: 1160 hours (diversion begins); B: 1338 hours; C: 1678.5 hours; D: 3029.5 hours.

Synthetic Example Monitoring with Surface ERI

Because the EKF has not been applied previously to surface ERI data, we test the method on a synthetic infiltration experiment to verify that the method works when measurement resolution is lower (because of acquistion geometry) than in previous cross-borehole applications. We begin by simulating an infiltration experiment by solving Richards equation numerically for a hydraulic head analysis using COMSOL. The structural model and values of hydrologic parameters used in the simulation are consistent with the current conceptual model

and available information about hydrologic properties of the HSRP, though the model here is downscaled from the pond. We simulate variably saturated fluid flow within the model space for 50 hours on an FEM grid of 5816 elements and 3609 nodes. The estimated effective saturation is output every hour. Effective saturation values are converted to conductivity values using an Archie's Law relationship with bulk fluid conductivity of 0.5 S/m, and cementation and saturation exponents of 1.5 and 2, respectively (Archie, 1940). The conductivity distributions at 1, 10, 20, and 30 hours simulated with this process are included in Figure 2 for reference.

Surface electrical resistivity measurements are simulated for 125 Wenner arrays using 40 electrodes and electrode offset spacing of 1:5 electrodes; data are then contaminated with 3% Gaussian noise. We note that, with the acquisition geometry used, the change in observed data between imaging experiments after 30 hours was less than the measurement noise. We, therefore, do not expect that inversion of these data will result in meaningful updates to the estimated conductivity structure.

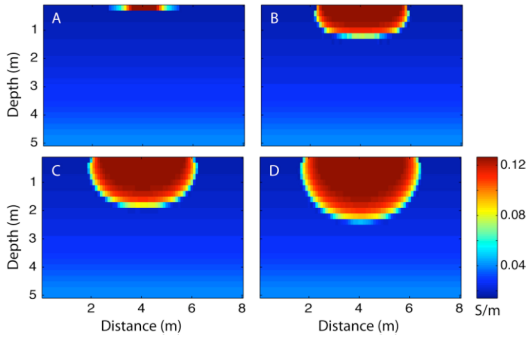

Figure 2: Four time-lapse conductivity models created based on the numerical solution to Richards equation for the effective saturation during an infiltration experiment and conversion to conductivity using an Archie's Law relationship. A: 1 hour; B: 5 hours; C: 20 hours; D: 30 hours.

We estimate the conductivity structure at each time step using the EKF prediction-filter recursions described above. We assume a model covariance of $1e0\mathbf{I}$; observation covariance of $2e\text{-}2\mathbf{I}$; and initial prediction error covariance matrix of the form $\mathbf{I}$. We assume a standard smoothing operator for R, with weighting coefficient equal to $\sqrt{2}$. Because time-steps are too small to allow distinguishable flow evolution between steps, we approximate $\mathbf{F}$ as the identity. This form of the state update incorporates our knowledge that the conductivity structure at any time-step should be close to the structure at the previous time-step, avoiding the computational expense of simulating the full solution of Richards equation at each time step and the assumption of several unknown values of hydrologic parameters. We use the same two-grid application described in the previous example. A fine grid of 320 by 100 cells is used to calculate the predicted data and Jacobian, while a coarse grid of 80 by 20 cells is used to update model parameters. Figure 3 shows the estimated conductivity models at time-steps consistent with the four conductivity distributions in Figure 2. The estimates show very good agreement with the 'true' structure, though the magnitudes of the conductivity values are very different from each other and the true models.

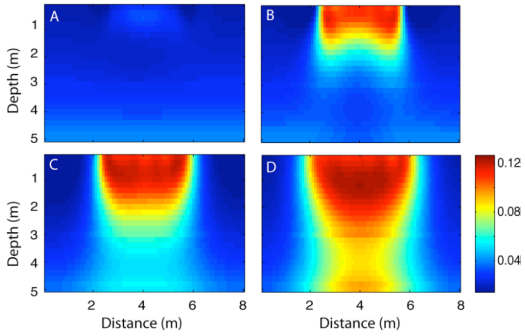

Figure 3: Four time-lapse conductivity models inverted using EKF. The models A-D correspond to the 'true' conductivity distributions A-D in Figure 2.

Conclusions

We present two methods for incorporating existing information from time-lapse ERI data into the inversion process within an informed imaging framework. Regularization of the inversion of the current estimate using prior estimates of the conductivity structure is applied to densely sampled monitoring data at an infiltration pond in Northern California. The extended Kalman Filter is shown to be a viable tool for the stochastic inversion of time-lapse surface ERI data. The recursive nature of the method allows for the incorporation of information from all previous imaging experiments into parameter estimation of the current experiment. Future investigation is required to determine the feasibility of applying the EKF to parameter estimation from continuous, automated ERI monitoring experiments.

Acknowledgements

This research was supported by funding to R. Knight from Schlumberger Water Services. We would like to thank Pajaro Valley Water Management Agency, particularly Brian Lockwood and Marry Bannister, for their assistance and support of this research.